Natural Hazards (2023) 119:2113–2131
https://doi.org/10.1007/s11069-023-06200-w

ORIGINAL PAPER

Investigation of past earthquakes in the Kopili fault zone, NE India: new evidence of paleoliquefaction

B. V. Lakshmi[1] · Md. Mujahed Baba[1] · Pravin B. Gawali[1]

Received: 11 February 2022 / Accepted: 4 September 2023 / Published online: 22 September 2023

Abstract

The Kopili fault (KF) zone, one of the active faults in northeastern region (NER), has experienced large earthquakes in 1869 (M_w 7.4) and 1943 (M_w 7.2). In order to mitigate future occurrences of earthquakes in the KF, it is essential to understand its long-term seismic history and seismic hazard implications. Seismogenic liquefaction features were identified at three trench sites in the floodplain deposits of Kolong River, near KF. The liquefaction features include multiple sand dykes and sand sills and are direct response to liquefaction of saturated sediment induced during past seismic activity. A total of seven samples from marker horizons have been processed to constrain the chronology of liquefaction features using optically stimulated luminescence (OSL) dating technique. OSL age constraints from Trench 1 indicate two episodes of earthquake-induced liquefaction since perhaps AD 1692, one, possibly two episodes of liquefaction in Trench 2 since AD 1540 and Trench 3, suggest one liquefaction event during the past 1000–2000 years. From the present study, given the limited results of the dating available we can conclude that two earthquakes induced liquefaction in the vicinity of the Kopili fault zone during the past ~ 480 years. Additional excavations and dating of earthquake-induced liquefaction features are required to precisely evaluate the frequency of major earthquakes in the KF zone.

Keywords Active fault · Earthquake · Kopili fault · Liquefaction features · Sand dyke · Sand sill

1 Introduction

One of the most useful secondary evidences in the category of seismically generated structures in the field of paleoseismology is liquefaction (Tuttle et al. 2019a, b). Liquefaction of saturated cohesionless sediments is caused by an increase in the pore water pressure due to the propagation of the cyclic shear waves during seismic shaking (Youd 1973, 1977; Sims 1973; Seed 1979; Obermeier 2009). Liquefaction is defined as transformation of a granular material from a solid to liquefied state due to increased pore water pressure. One of the main mechanisms, which produce liquefaction, is the cyclic shear stress/strain induced by

✉ B. V. Lakshmi
lakshmi.bv@iigm.res.in; lakshmi.nadiminty@gmail.com

1 Indian Institute of Geomagnetism, Kalamboli Highway, New Panvel, Navi Mumbai 410218, India

earthquakes. Liquefaction occurs mostly in soft sedimentary sequences especially interbedded sand and silt or clay; pebbly sand is difficult to liquefy, but pebbles can be entrained in escaping or venting water (Tuttle et al. 2019a, b). The liquefaction structures include sand dykes, sand blows, sand veins, pseudonodules, convolute bedding, load structure, diapirs, etc. There are several well-known examples of earthquakes of $M<5$ that have induced liquefaction (e.g., October 2010, M 4.8, Christchurch, NZ earthquake). The current state of knowledge is that earthquakes as small as M 4.5 can trigger liquefaction in sediment that is very susceptible to liquefaction (e.g., Green and Bommar 2019) and the factors that control the liquefaction are lithology, depth to the water table, epicentral distance, magnitude, earthquake duration, ground acceleration and amplitude of cycles (Seed 1979; Obermeier 1996; Moretti et al. 1999). Several studies have used liquefaction features as proxies in various geological and tectonic settings to investigate the seismic history (e.g., Russ 1982; Talwani and Cox 1985; Sims and Garvin 1995; Obermeier 1998, 2009; Sukhija et al. 1999; Tuttle et al. 2002, 2006; Rajendran et al. 2004; Villamor et al. 2016; Tuttle et al. 2019a, b).

The northeastern region (NER) of India has experienced high-magnitude earthquakes due to the ongoing collision of the Indian plate with the Eurasian plate to the north and Burmese plate to the east (Ambraseys and Douglas 2004; Bilham 2004), and the continual tectonics can potentially lead to more seismic activity. Hence, comprehending the frequency of major earthquakes is an important issue that can be addressed by focusing on evidence of the paleoearthquakes in the tectonically active regions. In the Himalaya, paleoseismic investigations have been carried out by trenching across primary fault scarps (e.g., Anand and Jain 1987; Jayangondaperumal and Thakur 2008; Kumar et al. 2010; Philip et al. 2011; Malik et al. 2015, 2017; Rajendran et al. 2015; Mishra et al. 2016; Jayangondaperumal et al. 2017; Priyanka et al. 2017; Pandey et al. 2021; Singh et al. 2021). Paleoseismic studies using liquefaction features (Sukhija et al. 1999; Singh and Jain 2007; Jayangondaperumal et al. 2008; Binita and Sharma 2009; Reddy et al. 2009; Morino et al. 2011; Singh et al. 2020; Jayangondaperumal 2021; Rajendran 2021; Lakshmi and Gawali 2022) and the historical earthquake catalogues (Bapat et al. 1983; Iyengar et al. 1999; Baro and Kumar 2017) suggested multiple seismic events to have occurred during the last millennium.

Where seismogenic faults are difficult to recognize, earthquake-induced liquefaction features have been the focus of a number of paleoseismological studies (e.g., Amick et al. 1990; Obermeier 1998; Saucier 1989; Tuttle and Seeber 1991; Tuttle and Atkinson 2010). Several well-known earthquakes, including the 1897 Assam earthquake (Oldham 1899) and the 1950 Upper Assam earthquake (Poddar1950), 1988 Saguenay, Quebec (Tuttle et al. 1990) and 2011 Christchurch, New Zealand earthquakes (Tuttle et al. 2017), induced liquefaction, but were not associated with surface rupture. These earthquakes raised the awareness that certain types of prehistoric earthquakes could not be identified by studying surface faults. Therefore, liquefaction features are used increasingly in paleoseismological investigations around the world, wherever sediments susceptible to liquefaction are present. Criteria for recognizing earthquake-induced liquefaction features from other types of soft sediment deformation structures already have been described in several papers (e.g., Sims 2012; Tuttle et al. 2019a, b and reference therein). Paleoseismic investigations of Kopili fault (KF) and in the Dauki fault (DF) in the meizoseismal area of the 1897 Assam and 1950 Upper Assam earthquakes revealed well-preserved liquefaction and deformed syndepositional features at selected sites in the alluvial deposits along the tributaries of the Brahmaputra River, Shillong plateau (SP), NER, India (Sukhija et al. 1999; Rajendran et al. 2004; Reddy et al. 2009; Kumar et al. 2016; Morino et al. 2011, 2014; Lakshmi and Gawali 2022).

Kumar et al. (2016) carried out paleoseismological studies using seismogenic liquefaction in the floodplain deposits of Kopili and Kolong Rivers. They excavated trenches at two locations and observed several sand dykes. In addition, they suggest three intervals of liquefaction formations using radiocarbon and OSL dating techniques. The paleoseismological record, however, provides only part of the data necessary to fully understand seismic hazard in the region. Observations of liquefaction features in the NER (Sukhija et al. 1999; Rajendran et al. 2004; Reddy et al. 2009) and accounts of liquefaction during historical earthquakes suggest that a history of paleoliquefaction events can be gleaned from the geological record that would shed light on the long-term behavior of the KF.

Here we present new evidence of sand dykes and sand sills resulted from the paleoearthquakes centered at KF region. In this paper, we intend to study paleoearthquake history in KF area by documenting and dating liquefaction features revealed in trenches.

2 Seismotectonics

The contiguous distribution and frequency of large intraplate earthquakes in India are poorly understood. The subduction of Indian plate under the Eurasian plate in the north brought Himalayan mountain ranges into picture while the eastern collision–subduction zone caused the existence of the Indo-Burma ranges (Fig. 1). As a result, the NER has a complex tectonic setting with a history of past large to great earthquakes (Ambraseys and Douglas 2004; Oldham 1899; Bilham 2004; Kayal 2008; Angelier and Baruah 2009). Four great earthquakes of magnitude (M) > 8.0 occurred in the last ca. hundred years: The 1897-Assam earthquake, 1905 Kangra earthquake, 1934 Bihar–Nepal earthquake and 1950 upper Assam earthquake occurred in NER (Fig. 1). The 300-km-long and 50-km-wide KF is seismically very active due to its transverse tectonics which places the region at risk for future large earthquakes (Kayal et al. 2012). The KF, which separates Shillong Plateau from the Mikir Hills, is one of the most important tectonic features of the NER. The KF is bounded by the Himalayan collisional zone in north, the Indo-Burmese subduction zone to the south, the syntaxis zone in the east and the SP in the west (Fig. 1). Many devastating earthquakes occurred in the past around the KF, viz. 1869 Cachar earthquake of M_w-7.4 (Oldham 1883), 1943 Hojai earthquake of M_w-7.2 (Nandy and Dasgupta 1991; Nandy 2001; Ambraseys and Douglas 2004), 1941 Tezpur earthquake of M-6.5 and 2009 Bhutan earthquake of M-6.9 (Kayal et al. 2012) (Figs. 1, 2).

3 Methods and research approach

Sites that liquefied during large modern earthquakes and historic earthquakes furnish good target for paleoliquefaction studies because liquefaction often reoccur where susceptible sediments are present (Tuttle et al. 2019a, b). Therefore, we have carried out investigation for liquefaction features along Kolong River near Namgaon, Satargaon and Nampani near KF in the eastern part of SP where ground failure and sand vents were reported during 1869 Cachar and 1943 Hojai earthquakes. Cut banks of the Kolong River were examined, during November and December 2016, for liquefaction and other soft sediment deformation structures, to assess spatiotemporal extent of strong shaking in KF (Figs. 3, 4, 5). We found, and have studied, many earthquake-induced liquefaction features along Kolong River. The information from sites is gathered from local knowledge by oral communication.

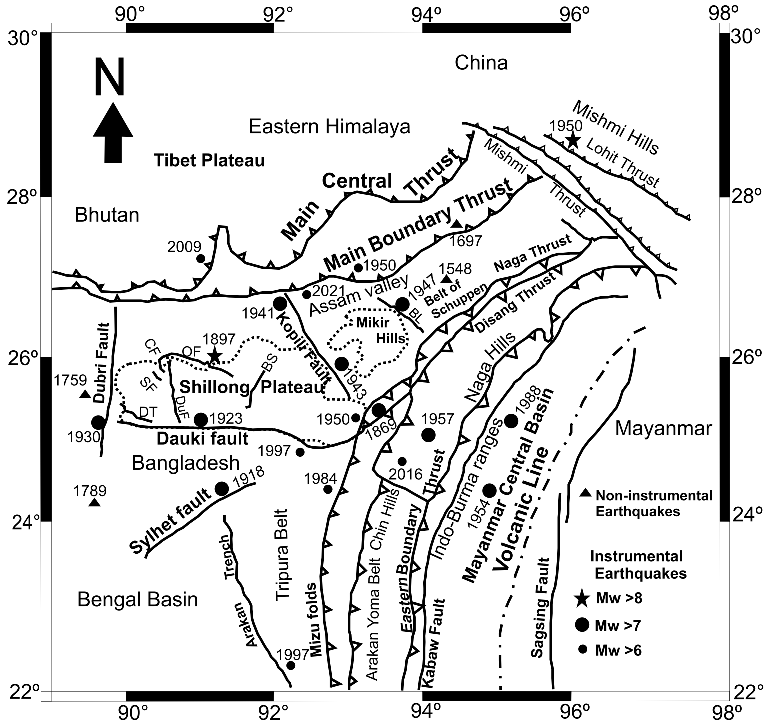

Fig. 1 Regional tectonic settings of northeast India and surrounding regions. *CF* Chedrang fault, *OF* Oldham fault, *SF* Samin fault, *DdF*: Dhudnoi fault, DT: Dapsi thrust, *BS*: Barapani shear zone, BL: Bomdila fault (Map sources: Murthy et al.1969; Nandy 2001; Angelier and Baruah 2009). Non-instrumental (Source: Iyengar et al. 1999) and instrumental earthquakes (Eq.) of magnitude ≥ 6 are plotted on the map (Sources: USGS and NCS, India). The Himalaya region has experienced four great earthquakes ($M > 8{:}0$) in the last ca. hundred years: 1897 Assam earthquake, Shillong Plateau, 1905 Kangra earthquake, 1934 Bihar–Nepal earthquake and 1950 Upper Assam earthquake. Black star depicts the two great earthquakes 1897 Shillong Eq. (M_w-8.1) and 1950 Assam Eq. (M_w-8.3) that are occurred in the northeastern region

We performed reconnaissance for liquefaction features in open fields and along river cut banks. We excavated features that appeared to be sand blows and cleaned cut banks to better reveal liquefaction features. We documented liquefaction features by logging exposures and collected sediment samples for OSL dating.

The sedimentary conditions of fluvial sand overlain by clay promote the increase in the pore water pressure during ground shaking which can lead to liquefaction (Tuttle et al. 2019a, b). Identification of liquefaction features in Brahmaputra flood plain is not always suitable due to monsoonal flooding and erosion by river during high flows. Consequently, during progressive excavation we observed liquefaction features, viz. several sand dykes (Figs. 3, 4, 5) as well as multiple dykes rising from the source layer of sand, mainly along and adjoining areas of the Kolong River, a tributary of Brahmaputra and in distal parts of the alluvial fans. Samples for optically stimulated luminescence (OSL) age determinations were collected from different stratigraphic levels to obtain maximum and minimum or contemporaneous ages of the liquefaction feature. The samples were collected in PVC tubes of 20 cm long and 2.5 cm diameter, and OSL dating was carried out by Wadia Institute of Himalayan Geology (WIHG), Dehradun (Table 1). Several studies have shown that at

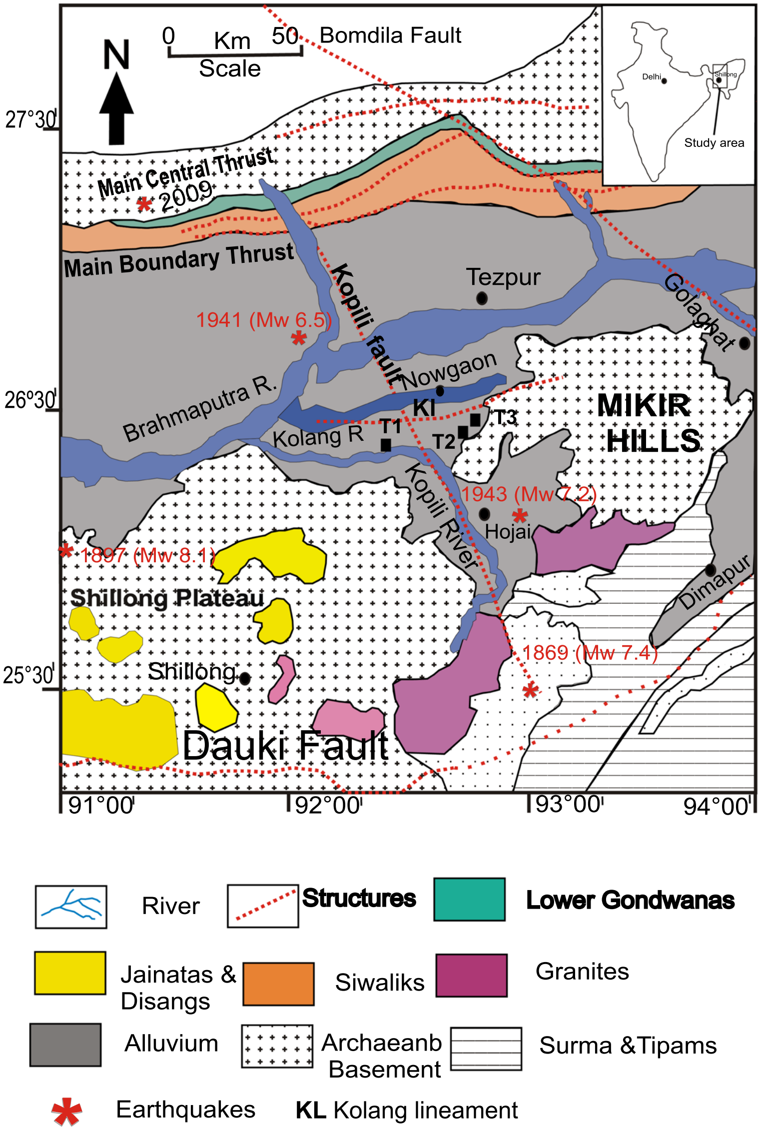

Fig. 2 Geological location map of the study trench sites along Kolong River, showing major structures (modified after Dasgupta 1977 and Nandy 2001). T1-Trench 1 at Namgaon site, T2-Trench 2 at Nampani site and T3-Trench 3 at Satargaon site. Epicenters of earthquakes that occurred in the Kopili fault region are plotted on the map

a given site recurring liquefaction corresponds to multiple earthquakes occurring at different time intervals (Youd 1977; Saucier 1989; Tuttle and Seeber1991; Obermeier 1998; Sims and Garvin 1995). Recurrent liquefaction can occur during an earthquake sequence (e.g., the 2010–2011 Canterbury earthquake sequence; Tuttle et al. 2017) or during earthquakes or earthquake sequences separated by hundreds of years [e.g., the New Madrid seismic zone (Tuttle et al. 2019a, b, 2002)]. The method to differentiate subsequent events

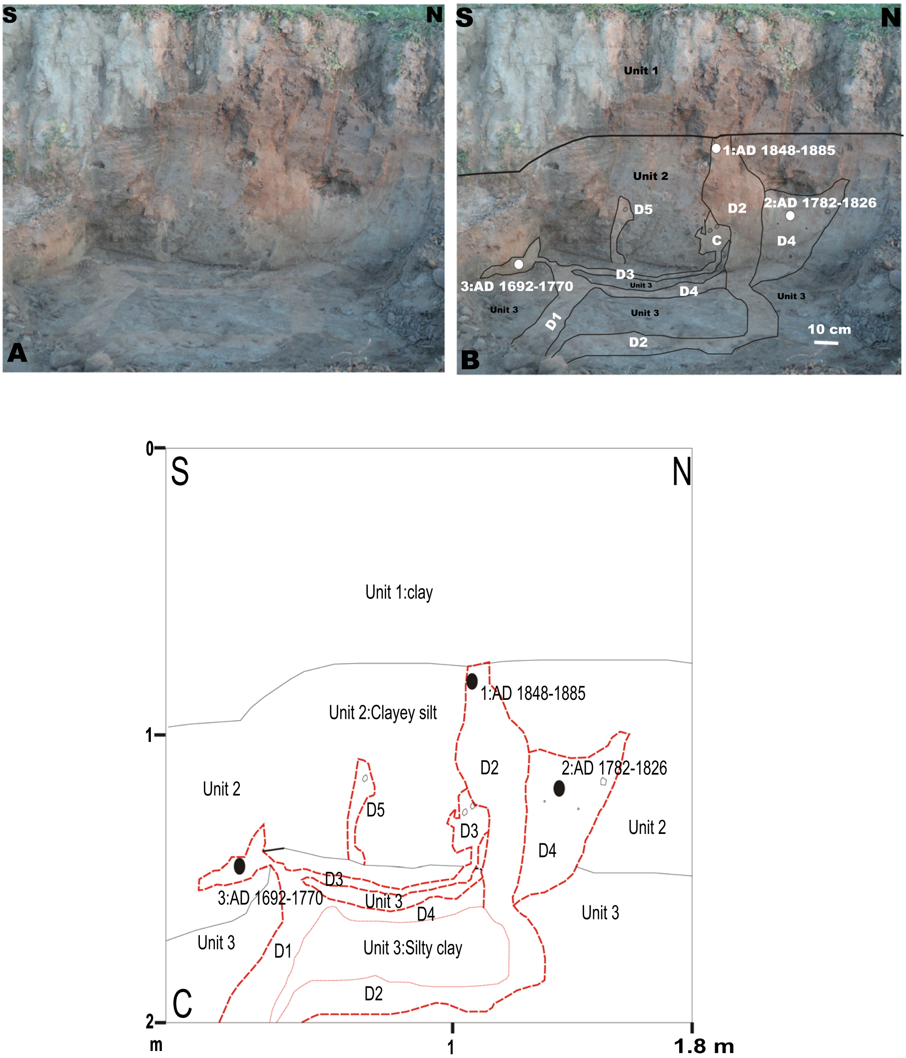

Fig. 3 Namgaon site (Trench 1) (N 26°12′50.5″; E 92°26′41.7″). **A** Uninterpreted and **B** interpreted Photograph of multiple sand dykes (D1, D2, D3, D4 and D5) in a ~ 1.8-m-long and ~ 2-m-deep Trench 1 section. **B** Two generation of main dykes D1 and D2 and D3 and D4 branched from D1 dyke. There is a second generation of sand dyke D2 that crosscuts D1, D3 and D4 dykes. The stratigraphic position and crosscutting relation of D3 dyke shows that it is older than D2 dyke and clearly indicates their formation in two distinct events which might have occurred within a short period of time. Another sand dyke D5 is terminated at 98 cm and no source sand layer observed. OSL date of AD 1692–1770 denotes the maximum age for Dyke D1, AD 1782–1826 provides maximum age for Dyke D4 and AD 1848–1885 provides maximum age for D2 dyke. From its stratigraphic position and OSL age data within the section, the D2 dyke represents more recent episode of liquefaction. Lithology of trench section consists of Unit 1: massive clay, Unit 2: clay–silt of light brownish gray color and Unit 3: gray color silt/clay. **C** Sketch highlighting the features exposed in the section in Trench 1

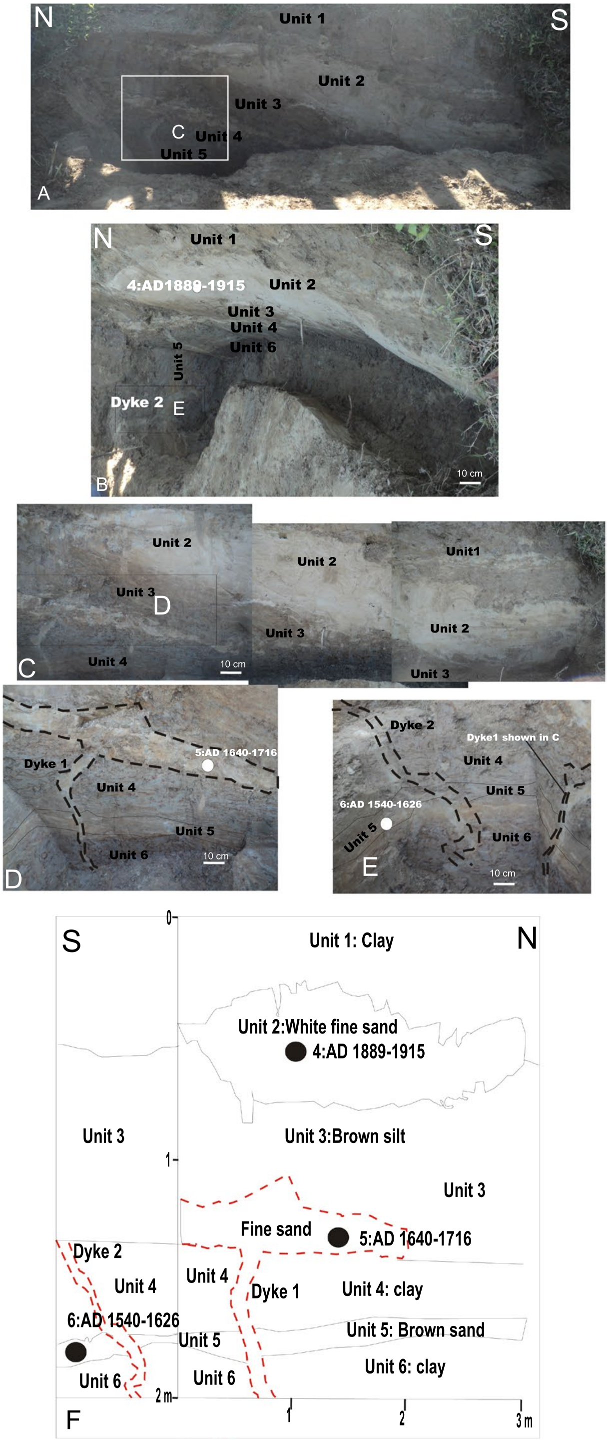

Fig. 4 Nampani site (Trench 2) (N 26°21′58″; E 92°46′38.7″). **A** Photograph of front view of Units 1–6 along with features in Trench 2 and **B** photograph of ~ 3-m-long and 2-m-deep Trench 2 showing two sand dykes. Age constraints were developed on the basis of OSL date within sand yielded age of AD 1889–1915 (115 ± 13). This age provides minimum age. Lithology of trench section consists of Unit 1: clay, Unit 2: sand, Unit 3: brown silt, Unit 4: sticky clay, Unit 5: sand and Unit 6: sticky clay. **C** Mosaic photograph details showing close-up view of sand sill and related sand dyke 1. **D** Photograph details showing sand sill and related sand dyke 1. **E** Photograph showing sand dykes 1 and 2. OSL age AD 1540–1626 (434 ± 43) of sample from this unit 5 provides maximum age. **F** Sketch highlighting the features exposed in the section from Trench 2

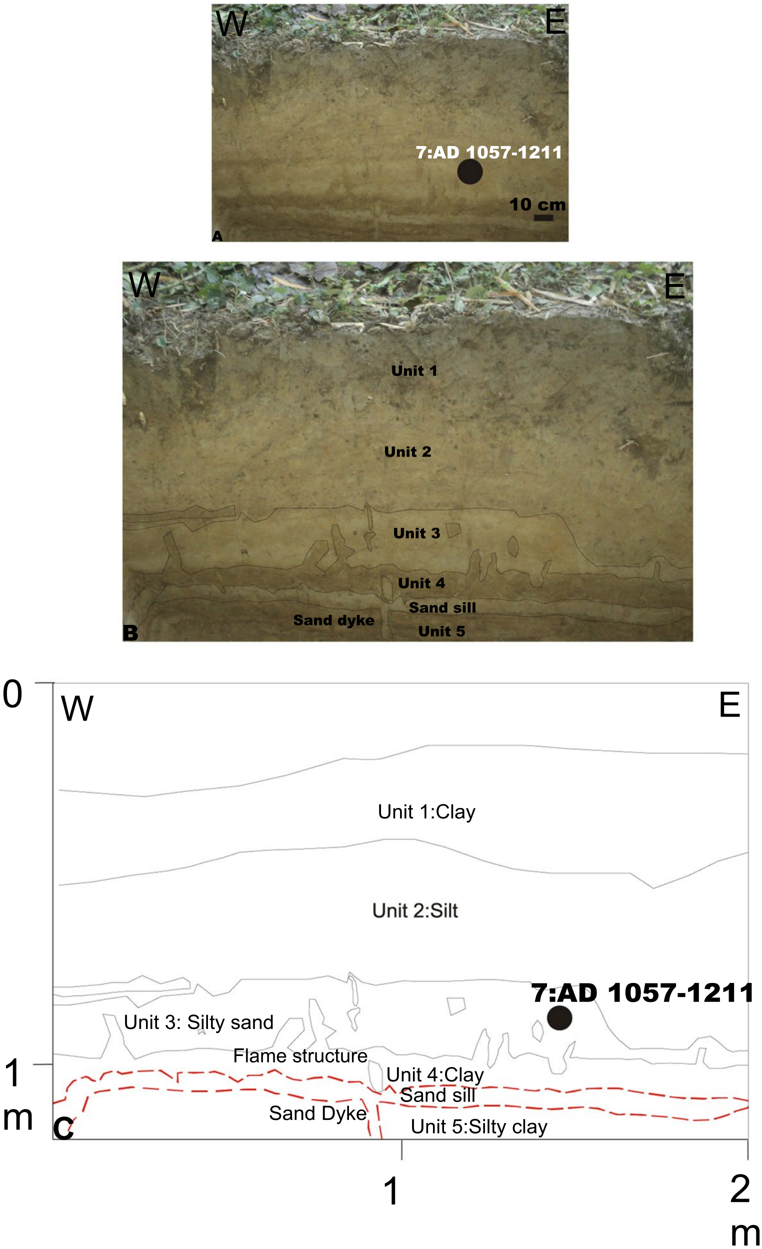

Fig. 5 Satargaon site (Trench 3) (N 26°23′12.5″; E 92°47′43.1). **A** Uninterpreted and **B** interpreted photograph of 2-m-long and 1.2-m-deep trench section showing sand sill and sand dyke. One main sand dyke, 5 cm wide, fed the SB. The dyke composed of fine light yellow sand, crosscutting Unit 5. A sand dyke have been observed in this section crossing the floor of the trench and continuing to be a sand sill intruded below clayey Unit 4. Sample collected above the sand dyke yielded OSL date of AD 1057–1211 (883 ± 77) provides minimum age constraint for the event. Lithology of trench section consists of Unit 1: clay, Unit 2: silt, Unit 3: brown silt–sand, Unit 4: clay, Unit and Unit 5: silt–clay. **C** Sketch of the section showing features

Table 1 Optically stimulated luminescence (OSL) ages of sediment samples (see Figs. 4, 5, 6 for sample location)

Lab no	Sample no/site no	Protocol	Depth cm	*K* (%)	*U* (ppm)	Th (ppm)	Mean equivalent dose (De) Gy	Dose rate (Gy/ka)	Age (yrs) (AD)
LD3120	1/NG/SB	DSAR	130	1.8	2.71	17.8	0.88 ± 0.1 (*n* = 5)	3.1 ± 0.3	286 ± 39 AD 1692–1770
LD3124	2/NG	SAR	100	1.7	3.13	14.2	0.65 ± 0.05 (*n* = 17)	3.0 ± 0.3	213 ± 22 AD 1782–1826
LD3122	3/NG	DSAR	80	2.3	1.38	23.7	0.54 ± 0.05 (*n* = 6)	3.6 ± 0.3	151 ± 18 AD 1848–1885
LD3123	4/NP	SAR	30	1.9	2.19	22.3	0.38 ± 0.03 (*n* = 17)	3.3 ± 0.3	115 ± 13 AD 1889–1915
LD3125	5/NP	DSAR	82	1.7	2.78	17.3	1.07 ± 0.09 (*n* = 17)	3.2 ± 0.3	339 ± 38 AD 1640–1716
LD3126	6/NP	DSAR	70	1.9	1.77	14.4	1.28 ± 0.08 (*n* = 20)	2.9 ± 0.3	434 ± 43 AD 1540–1626
LD3121	7/SG	SAR	57	2.5	3.52	28.0	3.9 ± 0.13 (*n* = 26)	4.4 ± 0.4	883 ± 77 AD 1057–1211

Optically stimulated luminescence (OSL) measurement were taken in an automated Riso TL/DA15 reader equipped with filtered green light from a halogen lamp, which is located at the Wadia Institute of Himalayan Geology, Dehra Dun, India. For the annual dose rate estimation, concentration of uranium, thorium and potassium in the sediments were measured by XRF. The single aliquot regeneration protocol (Murray and Wintle 2000) was used for equivalent dose determination. Water content assumed: 15 ± 5% by weight. 35 aliquots were used per samples. However, for LD3120 and 3122, 70 disk each were analyzed. For De calculation aliquots with recycling ratio within 10% were considered, n represents the number of aliquots qualified the criteria and considered in ED estimation. Over dispersion for all the samples was less than 20; hence, mean age model was used for paleodose estimation of liquefaction is typically based on the weathering characteristics, stratigraphic criteria, crosscutting and structural relationships, and dating of liquefaction features.

4 Results of investigations

Results of the search for and dating of liquefaction features along Kolong River, near KF region, are summarized in Table 1 and illustrated in Figs. 3, 4 and 5. Along Kolong River, we found ten liquefaction features in three trenches at three sites Namgaon (NG; Trench 1) Nampani (NP; Trench 2) and Satargaon (SG; Trench 3) (Fig. 2). Liquefaction features include sand dykes up to 23 cm wide and sand sills. The documented liquefaction features and their age constraints are discussed below.

4.1 Namgaon site

A ~ 1.8-m-long and ~ 2-m-deep Trench 1 was excavated along Kolong River at Namgaon (N 26°12′50.5″; E 92°26′41.7″), which consists of three visually distinguishable clay, silty sand, fine to medium sand and silty clay beds of varying thickness and have been designated as Units 1, 2 and 3 from top to bottom (Fig. 3A, B). Unit 1 consists of thick massive clay and Unit 2 consists of clay–silt of light brownish gray color with dykes intruding into it and the underlying Unit 3 consists of gray silt/clay. In this section, five dykes are documented and labeled as D1, D2, D3, D4 and D5 (Fig. 3A). These dykes range from 25 to 55 cm high and 5 to 20 cm wide. The two small dykes (D3 and D4) branch off of D1 dyke (Fig. 3B), D2 crosscuts D1, D3 and D4, and therefore, D2 represents a second episode of liquefaction. D3 and D4 branch off of D1 so apparently formed at the same time. They are composed predominately of fine to medium sand. D2 appears to have been truncated prior to deposition of Unit 1. So, dating of the base of Unit 1 provides a minimum constraining age for D2. The two dykes D3 and D4 terminate in the host deposit at 110 and 95 cm from the ground surface and younger D2 dyke at 80 cm, respectively. The stratigraphic position and crosscutting relation of D1, D3 and D4 dykes shows that they are older than D2 dyke and clearly indicates their formation in two distinct events which might have occurred within a short period of time. A small Dyke D5 25 cm high and 5 cm wide was observed only in Unit 2, where it terminates at ~ 98 cm below the top of the trench. D3, D4 and D5 terminate approximately at the same depth. Age constraints were developed on the basis of three OSL dates: AD 1848–1885 (151 ± 18), AD 1782–1826 (213 ± 22 years) and AD 1692–1770 (286 ± 39 years). Since the sand dikes were not exposed to the sun post-intrusion, the OSL dates of dike fill likely reflect the age of the source sand perhaps mixed with some of the host sediment. From the presented study, the data observations indicate two generations of liquefaction features that formed during two earthquakes. OSL dating of the sand dike lowest in the section might provide maximum age constraint of AD 1692 for the two generations of liquefaction features.

4.2 Nampani site

Trench 2 near Nampani village (N 26°21′58″; E 92°46′38.7″) revealed a 3-m-long and 2-m-deep sedimentary section consisting of white sand layers, brown sand and clay (Fig. 4A). Six distinct beds are identified in this trench walls. The 25–30-cm-thick Unit 1 constituted of clay, and the underlying Unit 2 consists of 50-cm-thick white fine sand. Unit

3 is of 35-cm-thick brown silt. Units 4 is ~ 10 cm thick and consists of sticky clay, and Unit 5 is up to ~ 5–15 cm thick and composed of fine brown sand. Unit 6 is 20–30 cm thick and consists of sticky clay. In this section, two sand dykes have been observed and labeled as Dyke 1 and Dyke 2, respectively. The two sand dykes Dyke 1 and Dyke 2 crosscut Units 4, 5 and 6 (Fig. 4D, F). Dyke 1 ranges from 50 cm high and 5–10 cm wide and crosscuts units 6, 5 and 4. Dyke 2, light yellow in color, also crosscuts units 6, 5 and 4 and attains a height of 60 and 5 cm width (Fig. 4D, F). The intruding slurry of water and entrained sand formed a sill of 10–30 cm thick along the contact between Units 3 and 5, and continued to intrude Unit 3 as a dike before it stopped. Age constraints were developed on the basis of three OSL dates, yielded ages of AD 1889–1915 (115 ± 13), AD 1640–1716 (339 ± 38) and AD 1540–1626 (434 ± 43), respectively (Fig. 4; Table 1). Observations indicate one generation of liquefaction features that formed during one earthquake, though a second event cannot be ruled out. OSL dating of Unit 6 provides maximum age constraint of AD 1540 for the liquefaction features.

4.3 Satargaon site

A 2-m-long and 1.2-m-deep trench was excavated at Satargaon site (N 26°23′12.5″; E 92°47′43.1). Six visually distinguishable layers of clay, silt and sand of varying thickness have been observed and designated as Units 1, 2, 3, 4 and 5 from top to bottom on the trench log (Fig. 5C). Unit 1 consists of 30-cm-thick clay, and Unit 2 composed of silt with thin interbedded clay. Unit 3 consists of 25-cm-thick irregular brown silty sand and thinning toward right side. Units 4 and 5 consist of clay and silty clay, respectively. A sand dyke has been observed in this section crossing the floor of the trench and continuing to be a sand sill intruded below clayey Unit 4 (Fig. 5A). The dyke composed of fine light yellow color sand, crosscutting unit 5. Sample collected within Unit 3 yielded OSL date of AD 1057–1211 (883 ± 77) (Table 1) and observations suggest they could have formed before or after AD 1057–1211. Given the age of the sediment exposed in the trench, the features probably formed during the late Holocene.

5 Discussions

5.1 Timing, sources and magnitude of paleoearthquakes

The stratigraphic criteria, geometry and crosscutting relations of deformational features provide evidence for repeated earthquake-induced liquefaction. The deformational features found in the present study, such as sand dikes and sand sills, are interpreted to earthquake-induced mechanism because their morphology indicates sudden application of a large upward-directed hydraulic force of short duration (Tuttle et al. 2019a, b) and presence of clasts. Similar features were observed in different geological and tectonic regimes during strong historical earthquakes (Obermeier 1996; Tuttle and Atkinson 2010; Mugnier et al. 2011; Cox et al. 2012, 2014; Tuttle et al. 2017) and have been reported earlier from different depositional environments in India including the Brahmaputra plains of NE India (Sukhija et al. 1999, 2002; Rajendran et al. 2004; Thomas et al. 2007; Jayangondaperumal and Thakur 2008; Reddy et al. 2009; Jayangondaperumal et al. 2011; Mugnier et al. 2011; Kumar et al. 2016; Lakshmi and Gawali 2022).

In the present study along Kolong River basin, the structural, stratigraphic and age relations at sites suggest that the paleoliquefaction features probably formed as the result of two event since AD 1540 or 450 yr BP (Table 1). Previous studies demonstrate that using OSL, 'direct dating' of prehistoric earthquakes may be possible, if sand blows or ground surface they buried resulting from subsurface liquefaction are preserved (Thomas et al. 2007; Porat et al. 2007). In our study, the sand dykes did not reached the ground surface, so their luminescence clock was not reset. Therefore, their OSL ages reflect the timing of the deposition of source sand assuming the source sand was exposed to sunlight long enough to reset its clock. The ages obtained from the present study grouped into two seismic events (Fig. 6). Observations from Namgaon Site, Trench 1, indicate two episodes of earthquake-induced liquefaction at Trench 1 since perhaps AD 1692. OSL dating of the sand dike lowest in the section might provide maximum age constraint of AD 1692 for the two generations of liquefaction features. Nampani Site, Trench 2 observations indicate one, possibly two episodes of liquefaction in Trench 2 since AD 1540. OSL dating of Unit 6 provides maximum age constraint of AD 1540 for the liquefaction features. Observations from Satargaon site, Trench 3, suggest one liquefaction event. The timing of the event is poorly constrained, but probably occurred sometime during the past 1000–2000 years. From the present study, given the limited results of the dating available (Table 1) we can conclude that two earthquakes induced liquefaction in the vicinity of the Kopili fault zone during the past ~ 480 years.

Instrumental records over the last five decade suggest that Cachar earthquake of 1869 (M_w-7.4) and Hojai earthquake of 1943 (M_w 7.2) occurred in the study area which was associated with the NW–SE trending KF (Figs. 1, 2) (Kayal et al. 2012). The only known historic earthquakes in this region capable of generating significant soil liquefaction are the 1869, the 1897, the 1941, the 1943, the 1950 and the 1697 earthquakes (Table 2). We first consider the 1697 Sadiya, 1897 and 1950 earthquakes which are 430, 210 and 310 km, respectively, quite far from the liquefaction feature in question (Table 2). Although it is tempting to compare with the earthquakes of AD 1697 Sadiya and AD 1950 Assam, these events are unlikely to have generated liquefaction, due to the distance to the assumed source. The 1897 Shillong earthquake (M_w 8.04) occurred on the Oldham fault (Bilham and England 2001) about 210 km away from the present study sites. According to the

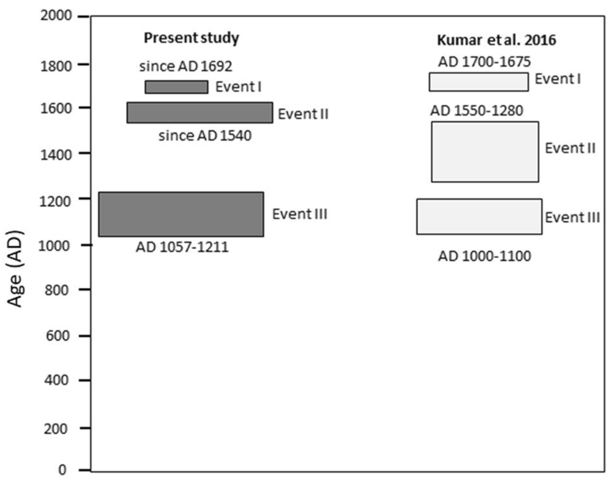

Fig. 6 Diagram showing the luminescence dates and preferred ages of the liquefaction episodes obtained from the present study sites

Table 2 List of the earthquakes, their magnitudes, distances from trenches (T1–T3) and their liquefaction susceptibility at the sites according to Castilla and Audemard (2007)

Historic earthquakes	Magnitude (M_w)	Distance from trenches (km)			Distance (Re) of earthquake to induce susceptible liquefaction according to $M_w = 2.44Log(Re) + 1.95$ (Castilla and Audemard (2007)	Liquefaction susceptibility
		T1	T2	T3		
1697 Sadiya	8.0	415	445	460	302	It will not induce liquefaction at the studied trenches
1869 Cachar	7.4	70	63	65	170	Likely to induce liquefaction at the studied trenches
1897 Assam	8.1	146	181	184	331	Likely to induce liquefaction at the studied trenches
1923 Meghalaya	6.5	168	206	209	73	It will not induce liquefaction at the studied trenches
1930 Dhubri	6.5	274	312	315	75	It will not induce liquefaction at the studied trenches
1941	6.5	25	55	50	73	Likely to induce liquefaction at the studied trenches
1943 Hojai	7.2	60	46	47	141	Likely to induce liquefaction at the studied trenches
1950 Assam	8.6	462	425	422	531	It will not induce liquefaction at the studied trenches

relation $M_w = 2.44$ Log (Re) + 1.95 (Castilla and Audemard 2007), the M 8.1, 1897 earthquake could induce liquefaction in very susceptible sediment up to a distance of ~ 331 km. Therefore, the 1897 earthquake could, but is not required, to have induced liquefaction at the three trench sites (Table 2). The 1869 event occurred in the southeastern end of the KF and has been well described by Oldham (1883) and about ~ 70 km away from the study sites. According to the relation $M_w = 2.44$ Log (Re) + 1.95 (Castilla and Audemard 2007), the 1869 M_w 7.4 earthquake could induce liquefaction in very susceptible sediment up to a distance of ~ 171 km. However, there is no large event in the KF since the 1943 M_w 7.2 Hojai earthquake. A comparison of the felt effects of the 1943 earthquake may be instructive at this point because this earthquake with the source at distance of 54 km from farthest liquefaction feature from the present study. According to the relation $M_w = 2.44$ Log (Re) + 1.95 (Castilla and Audemard 2007), the 1943 M_w 7.2 Hojai earthquake could induce liquefaction in very susceptible sediment up to a distance of ~ 141 km. It would appear that several historical earthquakes including the 1943, 1941, 1897 and 1869 earthquakes might be capable of inducing liquefaction at the trench sites (Table 2). This will, however, remain a tentative conclusion until we develop more rigorous age constraints from future studies of paleoliquefaction features in this region. In addition, liquefaction potential studies of sediments at the sites would help to determine which of the historical earthquakes would be more likely to be responsible for liquefaction.

Kumar et al. (2016) dated the liquefaction feature that occurred about 900 yr BP at the Kakotigaon along Kolong River which is 30 km from the present study sites. These data suggest that the liquefaction event at Satargaon site might correspond to 900 yr BP, but only one observation supports this conclusion (Fig. 6). Dating of more paleoliquefaction features at additional sites in the KF would greatly improve our determination of the timing and the likely seismic source of the causative earthquakes.

In the past, the KF has experienced several earthquakes of magnitude 4.5–6.2, three of magnitude 6 to 7 and two earthquakes of magnitude greater than 7, viz. 1869 Cachar and 1943 Hojai earthquakes. This region has been identified as a probable region for future large magnitude earthquakes (Kayal et al. 2006, 2010, 2012). Recently, it is argued that KF cuts across the Himalayas and caused displacement and curvilinear structure at the main boundary fault and main central thrust zones (Kayal et al. 2010, 2012). Paleoseismic investigation in the KF by Kumar et al. (2016) revealed seismogenic liquefaction features near Kopili and Kolong Rivers which correspond to the occurrence of three (250 ± 25 yr BP, between 400 and 700 yr BP and 900 ± 50 yr BP) causative seismic events (Fig. 6). However, both the studies, Kumar et al. (2016) and the present study, indicate that 1943 earthquake of comparable magnitude occurred in the Assam, which has generated liquefaction features of similar dimensions in the source zone nearby KF. But there is also a possibility that even a distant great earthquake could generate liquefaction in the KF. As it is restricted to only a few sites, the present study cannot resolve on the estimates of earthquakes sizes, nor can it resolve the source zones. In the present study, we made an attempt to provide a tentative time series of earthquakes that impacted a part of the Kopili alluvial plains. The limited dating constraints based on only a few liquefaction features are presented here and are less than sufficient to develop a timeline of earthquakes that impacted the KF. Scores of broadly distributed liquefaction sites should be studied in order to determine with confidence the timing and source area(s) of the causative earthquakes.

The magnitude of the earthquake that induced the observed liquefaction features is estimated on the basis of relation, inferred epicenter to the farthest site where liquefaction was observed. Comparison of shallow-focus events worldwide has shown that there is a well-defined upper limit of radius of liquefaction (Ambraseys 1988). Assuming an epicenter near Kopili fault, the greatest epicentral distance is 37 km (site NG to site NP). Using Ambraseys (1988), an estimate of *M* 6.4 is indicated for the events that caused thee liquefaction. If the Kopili fault were the source, an earthquake as small as *M* 6.4 could be responsible for liquefaction at all three study sites. A much larger earthquake from the same source induces liquefaction at other sites at much greater distances as well as at the study sites. Our analysis suggests that historical earthquakes in the region could have been responsible for liquefaction at the sites. So the question becomes how you can distinguish liquefaction from a local earthquake produced by the Kopili fault and liquefaction from the historical earthquakes. It would be a big job, involving studying and dating many liquefaction features across the region and mapping the liquefaction fields related to the different earthquakes.

As additional liquefaction features are found and dated, liquefaction fields and thus epicentral distances to farthest liquefaction features are likely to increase, leading to greater magnitudes estimates.

6 Conclusions

A wealth of information regarding paleoearthquakes is accessible in the form of seismically induced liquefaction features preserved in the alluvial deposits along Kolong River near KF region. During our paleoseismic investigation, we found liquefaction features and included sand dikes and sand sills at sites Namgaon (NG), Nampani (NP) and Satargaon (SG). The OSL ages correspond to two episodes of earthquake-induced liquefaction since perhaps AD 1692; one, possibly two episodes of liquefaction since AD 1540; and another episode of liquefaction sometime in the past 1000–2000 years. On the basis of OSL dating, we interpret that the two earthquakes that caused induced liquefaction in the vicinity of the Kopili fault zone during the past ~ 480 years. Several fault zones in the SP, including the DF, Oldham fault, Dapsi thrust and KF are thought to be active on the basis of their apparent influence on local topography and hydrography. Additional investigations of liquefaction features are needed to provide better constrains on timing, magnitude and sources of paleoearthquakes in the KF. These details in turn will help in interpretation of long-term rupture history of faults and intraplate seismicity. Eventually, the present study demonstrates that the paleoseismic investigations can provide useful information on past earthquakes through recognition of liquefaction features in the absence of surface rupture. Paleoseismic approach also contributes data on unknown seismic events in seismically active region like SP.

Acknowledgements The authors are grateful to Director, IIG, for his support and necessary permission for publishing this paper. We acknowledge financial support from CLAIMs in house program of DST-IIG. We are most grateful to two anonymous reviewers for their careful reading of our manuscript, and their many insightful comments and suggestions helped improve the manuscript. We also thank Prof. Harsh K. Gupta, Editor-in-Chief, for his suggestions and continuous support. The author Praveen Gawali who have contributed substantially for this article expired on January 22, 2022, prior to the submission of this paper.

Funding This is DST-IIG funded in house CLAIMS Project.

Declarations

Conflict of interest The authors declare that they have no known competing financial interests or personal relationships that could have appeared to influence the work reported in this paper.

References

Ambraseys NN (1988) Engineering seismology. Earthq Eng Struct Dyn 17:1–105

Ambraseys NN, Douglas J (2004) Magnitude calibration of north Indian earthquakes. Geophys J Int 159:165–206

Amick D, Gelinas R, Maurath G, Cannon H, Moor D, Billington E, Kempinen H (1990) Paleoliquefaction features along the atlantic seabord, U.S.N.R.C, Washington DC 20555 NRC FIN D 1682. NUREG/CR-5613 RA

Anand A, Jain AK (1987) Earthquakes and deformational structures (seismites) in Holocene sediments from the Himalayan-Andaman Arc, India. Tectonophysics 133:105–120

Angelier J, Baruah S (2009) Seismotectonics in Northeast India: a stress analysis of focal mechanism solutions of earthquakes and its kinematic implications. Geophys J Int 178:303–326

Bapat A, Kulkarni RC, Guha SK (1983) Catalogue of earthquakes in India and neighbourhood: from historical period up to 1979. Indian Society of Earthquake Technology, Roorkee, p 211p

Baro O, Kumar A (2017) Seismic source characterization for the Shillong plateau in Northeast India. J Seismol 21:1229–1249

Bilham R (2004) Earthquakes in India and the Himalaya: tectonics, geodesy and history. Ann Geophys 47:839–858

Bilham R, England P (2001) Plateau pop up in the great 1897 Assam earthquake. Nature 410:806–809

Binita P, Sharma A (2009) Soft-sediment deformation structures in the Late Quaternary sediments of Ladakh: evidence for multiple phases of seismic tremors in the North western Himalayan Region. J Asian Earth Sci 34:761–770

Castilla RA, Audemard FA (2007) Sand blows as a potential tool for magnitude estimation of pre-instrumental earthquakes. J Seismolog 11:473–487

Cox RT, Harris JB, Forman SL, Brezina T, Gordon J, Gardner C (2012) Holocene faulting on the Saline River fault zone, Arkansas, along the Alabama-Oklahoma transform. In: Cox RT, Tuttle MP, Boyd OS, Locat J (eds) Recent advances in North American paleoseismology and neotectonics east of the rockies. Geol Soc Am Spec Paper, vol 493, pp 143–174

Cox RT, Lowe C, Hao Y, Mahan SA (2014) Use of small scale liquefaction features to assess paleoseismicity: an example from the Saline River fault zone, Southeast Arkansas, USA. Front Earth Sci 2:1–17

Dasgupta AB (1977) Geology of Assam Arakan region. Mining Metall Soc India Q J 49:1–54

Green RA, Bommar J (2019) What is the smallest earthquake magnitude that needs to be considered in assessing lifuefaction hazard. Earthq Spectra 35:1441–1464

Iyengar RN, Sharma D, Siddiqui JM (1999) Earthquake history of India in medieval times. Indian J His Sci 34(3):181–237

Jayangondaperumal R (2021) Geological Evidence of Great Earthquakes along the Eastern Himalayan Foothills. J Geol Soc India 97:823–926

Jayangondaperumal R, Thakur VC (2008) Co-seismic secondary surface fractures on southeastward extension of the rupture zone of the 2005 Kashmir earthquake. Tectonophysics 446:61–76

Jayangondaperumal R, Thakur VC, Suresh N (2008) Liquefaction features of the 2005 Muzaffarabad-Kashmir earthquake and evidence of paleoearthquakes near Jammu Kashmir Himalaya. Curr Sci 95:1071–1076

Jayangondaperumal R, Wesnousky SG, Choudhuri BK (2011) Near-surface expression of early to late Holocene displacement along the northeastern Himalayan frontal thrust at Marbang Korong Creek, Arunachal Pradesh, India. Bull Seismol Soc Am 101(6):3060–3066

Jayangondaperumal R, Kumahara Y, Thakur VC, Srivastava AKP, Shubhanshu D, Joe V, Dubey AK (2017) Great earthquake surface ruptures along back thrust of the Janauri anticline, NW Himalaya. J Asian Earth Sci 133:89–101

Kayal JR (2008) Microearthquake seismology and seismotectonics of South Asia. McGraw Hill Publication, India

Kayal JR, Arefie SS, Barua S, Hazarika D, Gogoi N, Kumar A, Chowdhury SN, Kalita S (2006) Shillong plateau earthquakes in northeast India region: complex tectonic model. Curr Sci 91:109–114

Kayal JR, Arefiev SS, Baruah S, Tatevossian R, Gogoi N, Sanoujam M, Gautam JL, Hazarika D, Borah D (2010) The 2009 Bhutan and Assam felt earthquakes (*M*w 6.3 and 5.1) at the Kopili fault in the northeast Himalaya region. Geomat Nat Haz Risk 1:273–281

Kayal JR, Arefiev SS, Baruah S, Hazarika D, Gogoi N, Gautam JL, Santanu B, Dorbath C, Tatevossian R (2012) Large and great earthquakes in the Shillong plateau–Assam valley area of northeast India region: pop-up and transverse tectonics. Tectonophysics 532–535:186–192

Kumar S, Wesnousky SG, Jayangondaperumal R, Nakata T, Kumahara Y, Singh V (2010) Paleoseismological evidence of surface faulting along the northeastern Himalayan front, India: timing, size, and spatial extent of great earthquakes. J Geophys Res 115:B12422
Kumar D, Reddy DV, Pandey A (2016) Paleoseismic investigations in the Kopili fault zone of North East India: evidences from liquefaction chronology. Tectonophysics. https://doi.org/10.1016/j.tecto.2016.02.016
Lakshmi BV, Gawali PB (2022) Soft sediment deformation features in Dauki Fault region: Evidence of paleoearthquakes, Shillong Plateau. NE India. Environ Earth Sci 81:58
Malik JN, Sahoo S, Satuluri S, Okumura K (2015) Active Fault and paleoseismic studies in Kangra Valley: evidence of surface rupture of a Great Himalayan 1905 Kangra Earthquake (*M*w 7.8), Northwest Himalaya India. Bull Seismol Soc Am 105:2325–2342
Malik JN, Naik SP, Sahoo S, Okumura K, Mohanty A (2017) Paleoseismic evidence of the CE 1505 (?) and CE 1803 earthquakes from the foothill zone of the Kumaon Himalaya along the Himalayan Frontal Thrust (HFT) India. Tectonophysics 714:133–145
Mishra RL, Singh I, Pandey A, Rao PS, Sahoo HK, Jayangondaperumal R (2016) Paleoseismic evidence of a giant medieval earthquake in the eastern Himalaya. Geophys Res Lett 43(11):5707–5715
Moretti M, Alfaro P, Caselles O, Canas JA (1999) Modelling seismites with a digital shaking table. Tectonophysics 304(4):369–383
Morino M, Kamal ASMM, Muslim D, Ali RMdE, Kamal MA, Rahman MdZ, Kaneko F (2011) Seismic event of the Dauki Fault in 16th Century confirmed by trench investigation at Gabrakhari Village, Haluaghat, Mymensingh, Bangladesh. J Asian Earth Sci 42:492–498
Morino M, Kamal ASMM, Akhter SH, Rahman MdZ, Ali RMdE, Talukder A, Khan MdMH, Matsuo J, Kaneko F (2014) A paleo-seismological study of the Dauki fault at Jaflong, Sylhet, Bangladesh: historical seismic events and an attempted rupture. J Asian Earth Sci 491:218–226
Mugnier JL, Huyghe P, Gajurel A, Upreti B, Jouanne F (2011) Seismities in the Kathmandu basin and seismic hazard. Tectonophysics 509:33–49
Murray A, Wintle A (2000) Luminescence dating of quartz using an improved single aliquot regenerative-dose protocol. Mater Sci 32:57–73
Murthy MVN, Talukdar SC, Batthacharya AC (1969) The Dauki fault of Assam. Bull Oil Nat Gas Comm 6:57–64
Nandy DR (2001) Geodynamics of Northeastern India and the adjoining region. ACB Publication, Kolkata, p 209
Nandy DR, Dasgupta S (1991) Seismotectonic domains of northeastern India and adjacent areas. Phys Chem Earth 18:371–384
Obermeier SF (1996) Use of liquefaction-induced features for paleoseismic analysis: an overview of how seismic liquefaction features can be distinguished from other features and how their regional distribution and properties of source sediment can be used to infer the location and strength of Holocene paleo-earthquakes. Eng Geol 44:1–76
Obermeier SF (1998) Liquefaction evidence for strong earthquakes of Holocene and Latest Pleistocene ages in the States of Indiana and Illinois, USA. Eng Geol 50:227–254
Obermeier SF (2009) Using liquefaction-induced and other soft-sediment features for paleoseismic analysis. In: McCalpin JP (ed) Paleoseismology, 2nd edn. Academic Press, London, pp 497–564
Oldham T (1883) The Cachar earthquake of 10th January 1869. Mem Geol Surv India 19:1–88
Oldham RD (1899) Report on the great earthquake of 12th June, 1897. Mem Geol Surv India 29:1–379
Pandey A, Jayangondaperumal R, Hetényi G, Priyanka SR, Singh I, Srivastava P, Srivastava HB (2021) Establishing primary surface rupture evidence and magnitude of the 1697 CE Sadiya earthquake at the Eastern Himalayan Frontal thrust. India Sci Rep 11(1):1–14
Philip G, Suresh N, Bhakuni SS, Gupta V (2011) Paleoseismic investigation along Nalagarh Thrust: evidence of Late Pleistocene earthquake in Pinjaur Dun, Northwestern sub-Himalaya. J Asian Earth Sci 40:1056–1067
Poddar MC (1950) The Assam earthquake of 15th August 1950. Indian Miner 4:167–176
Porat N, Levi T, Weinberger R (2007) Possible resetting of quartz OSL signals during earthquakes-evidence from late Pleistocene injection dikes, Dead Sea basin, Israel. Quat Geochronol 2:272–277
Priyanka RS, Jayangondaperumal R, Pandey A, Mishra RL, Singh I, Bhushan R et al (2017) Primary surface rupture of the 1950 Tibet-Assam great earthquake along the eastern Himalayan front. India Sci Rep 7(1):1–12
Rajendran CP (2021) Constraints on previous earthquakes from the liquefaction sites in the Kathmandu Valley associated with the 2015 Gorkha earthquake and their regional implications. Quat Int 585:44–54

Rajendran CP, Rajendran K, Duarah BP, Baruah S, Earnest A (2004) Interpreting the style of faulting and paleoseismicity associated with the 1897 Shillong, northeast India, earthquake: implications for regional tectonism. Tectonics 23(4):1–12

Rajendran CP, John B, Rajendran K (2015) Medieval pulse of great earthquakes in the central Himalaya: viewing past activities on the frontal thrust. J Geophys Res Solid Earth 120:1623–1641

Reddy DV, Nagabhushanam P, Kumar D, Sukhija BS, Thomas PJ, Pandey AK, Sahoo RN, Ravi Prasad GV, Datta K (2009) The great 1950 Assam Earthquake revisited: field evidences of liquefaction and search for paleoseismic events. Tectonophysics 474:463–472

Russ DP (1982) Style and significance of surface deformation in the vicinity of New Madrid, Missouri. In: McKeown FA, Pakiser LC (eds) Investigations of the New Madrid, Missouri, Earthquake Region. U. S. Geol Survey Prof. Paper, vol 1236, pp 95–114

Saucier RT (1989) Evidence for episodic sand-blow activity during the 1811–1812 New Madrid (Missouri) Earthquake Series. Geology 17:103–106

Seed HB (1979) Soil liquefaction and cyclic mobility evaluation for level ground duringearthquakes. Proc Am Soc Civil Eng J Geotech Eng 105:201–255

Sims JD (1973) Earthquake induced structures in sediments of Van Norman Lake, San Fenando, California. Science 182:161–163

Sims JD (2012) Earthquake-induced laod casts, pseudonodules, Ball-and-pillow, and Convolute Lamination: Additional Deformation Structures for Paleoseismic studies. In: Cox RT, Tuttle MP, Boyd OS, Locat J (eds) Recent advances in North American paleoseismology and neotectonics east of the rockies. Geol Soc Am Spec Paper 493

Sims JD, Garvin CD (1995) Recurrent liquefaction induced by the 1989 Loma Prieta earthquake and 1990 and 1991 aftershocks: implications for paleoseismicity studies. Bull Seism Soc Am 85:51–65

Singh S, Jain AK (2007) Liquefaction and fluidization of lacustrine deposits from Lahaul-Spiti and Ladakh Himalaya: geological evidences of palaeoseismicity along active fault zone. Sediment Geol 196:47–57

Singh BP, Mondal K, Singh A, Mittal Singh RK, Kanhaiya S (2020) Seismic origin of the soft-sediment deformation structures in the upper Palaeo-Mesoproterozoic Semri Group, Vindhyan Supergroup, Central India. Geol J 55(11):1–15

Singh I, Pandey A, Mishra RL, Priyanka RS, Brice A, Jayangondaperumal R, Srivastava V (2021) Evidence of the 1950 great Assam earthquake surface break along the Mishmi Thrust at Namche Barwa Himalayan Syntaxis. Geophys Res Lett 48:e2020GL090893

Sukhija BS, Rao MN, Reddy DV, Nagabhushanam P, Hussain S, Chadha RK, Gupta HK (1999) Paleoliquefaction evidence and periodicity of large prehistoric earthquakes in Shillong Plateau, India. Earth Planet Sci Lett 167:269–282

Sukhija BS, Rao MN, Reddy DV, Nagabhushanam P, Kumar D, Lakshmi BV, Sharma P (2002) Palaeoliquefaction evidence of prehistoric large/great earthquakes in north Bihar, India. Cur Sci 83:1019–1025

Talwani P, Cox J (1985) Paleoseismic evidence for recurrence of earthquakes near Charleston, South Carolina. Science 229:379–381

Thomas PJ, Reddy DV, Kumar D, Nagabhushanam P, Sukhija BS, Sahoo RN (2007) Optical dating of liquefaction features to constrain prehistoric earthquakes in Upper Assam, NE India-some preliminary results. Quat Geochronol 2:278–283

Tuttle MP, Atkinson GM (2010) Localization of large earthquakes in the Charlevoix seismic zone, Quebec, Canada, during the past 10,000 years. Seism Res Lett 81:140–147

Tuttle MP, Seeber L (1991) Historic and prehistoric earthquakeinduced liquefaction in Newbury, Massachusetts. Geology 19:594–597

Tuttle M, Law T, Seeber L, Jacob K (1990) Liquefaction and ground failure in Ferlamd, Quebec, triggered by the 1988 Saguenay Earthquake. Can Geotech J 27:580–589

Tuttle MP, Schweing ES, Sims JD, Lafferty RH, Wolf LW, Haynes ML (2002) The Earthquake potential of New Madrib seismic zone. Bull Seismol Soc Am 92:2080–2089

Tuttle MP, Shukri HA, Mahdi H (2006) Very large earthquakes centered southwest of the New Madrid seismic zone 5000–7000 years ago. Seism Res Lett 77:664–678

Tuttle MP, Villamor P, Almond P et al (2017) Liquefaction induced during the 2010–2011 Canterbury, Newzealand, earthquake sequence and lessons learned for the study of paleoliquefaction feature. Seismol Res Lett 88:1403–1414

Tuttle MP, Wolf LW, Starr ME, Villamor P, Mayne PW, Lafferty RH III, Morrow JE, Scott RJ Jr, Forman SL, Hess K, Tucker K, Dunahue J, Haynes ML (2019a) Evidence for large New Madrid earthquakes about AD 0 and BC 1050, Central United States. Seismol Res Lett 90:1393–1406

Tuttle MP, Hartleb R, Wolf L, Mayne PW (2019b) Paleoliquefaction studies and the evaluation of seismic hazard. Geosciences 9:2–61
Villamor P, Almond P, Tuttle MP et al (2016) Liquefaction Features Produced by the 2010–2011 Canterbury Earthquake Sequence in Southwest Christchurch, New Zealand, and Preliminary Assessment of Paleoliquefaction Features. Bull Seismol Soc Am 106:1–25
Youd TL (1973) Liquefaction, flow, and associated ground failure. US Geol Surv Circ 688:1–12
Youd TL (1977) ‘‘Discussion of “Brief review of liquefaction during earthquakes in Japan” by Kuribayashi, E. and Tatsuoka, F., 1975, in Soil and Foundations 15, 81–92. Soils Foun 17:82–85